ISSN 1674-1056
http://cpb.iphy.ac.cn
http://iopscience.iop.org/cpb
中国物理 B
Chinese Physics
中国物理 Chinese Physics B

A general method for large-scale fabrication of Cu nanoislands/dragonfly wing SERS flexible substrates

Yuhong Wang(王玉红), Mingli Wang(王明利), Lin Shen(沈琳), Yanying Zhu(朱艳英), Xin Sun(孙鑫), Guochao Shi(史国超), Xiaona Xu(许晓娜), Ruifeng Li(李瑞峰), Wanli Ma(马万里)
Citation: Chin. Phys. B . 2018, 27(1): 017801. **doi:** 10.1088/1674-1056/27/1/017801

Journal homepage: http://cpb.iphy.ac.cn; http://iopscience.iop.org/cpb

What follows is a list of articles you may be interested in

Effects of the ion-beam voltage on the properties of the diamond-like carbon thin film prepared by ion-beam sputtering deposition

Sun Peng, Hu Ming, Zhang Feng, Ji Yi-Qin, Liu Hua-Song, Liu Dan-Dan, Leng Jian
Chin. Phys. B . 2015, 24(6): 067803. **doi:** 10.1088/1674-1056/24/6/067803

Three-dimensional noble-metal nanostructure：A new kind of substrate for sensitive, uniform, and reproducible surface-enhanced Raman scattering

Tian Cui-Feng, You Hong-Jun, Fang Ji-Xiang
Chin. Phys. B . 2014, 23(8): 087801. **doi:** 10.1088/1674-1056/23/8/087801

Thickness dependence of the optical constants of oxidized copper thin films based on ellipsometry and transmittance

Gong Jun-Bo, Dong Wei-Le, Dai Ru-Cheng, Wang Zhong-Ping, Zhang Zeng-Ming, Ding Ze-Jun
Chin. Phys. B . 2014, 23(8): 087802. **doi:** 10.1088/1674-1056/23/8/087802

An effective surface-enhanced Raman scattering template based on gold nanoparticle/silicon nanowire arrays

Wang Ming-Li, Zhang Chang-Xing, Wu Zheng-Long, Jing Xi-Li, Xu Hai-Jun
Chin. Phys. B . 2014, 23(6): 067802. **doi:** 10.1088/1674-1056/23/6/067802

Enormous enhancement of electric field in active gold nanoshells

Jiang Shu-Min, Wu Da-Jian, Wu Xue-Wei, Liu Xiao-Jun
Chin. Phys. B . 2014, 23(4): 047807. **doi:** 10.1088/1674-1056/23/4/047807

A general method for large-scale fabrication of Cu nanoislands/dragonfly wing SERS flexible substrates*

Yuhong Wang(王玉红)[1], Mingli Wang(王明利)[1,†], Lin Shen(沈琳)[2], Yanying Zhu(朱艳英)[1], Xin Sun(孙鑫)[1], Guochao Shi(史国超)[1], Xiaona Xu(许晓娜)[1], Ruifeng Li(李瑞峰)[1], and Wanli Ma(马万里)[3]

[1] *Key Laboratory for Microstructural Material Physics of Hebei Province, School of Science, Yanshan University, Qinhuangdao* 066004, *China*
[2] *Liren College of Yanshan University, Qinhuangdao* 066004, *China*
[3] *Department of Mathematics, NC State University, Raleigh* 276968205, *USA*

(Received 21 May 2017; revised manuscript received 24 September 2017; published online 28 November 2017)

Noble metal nanorough surfaces that support strong surface-enhanced Raman scattering (SERS) is widely applied in the practical detection of organic molecules. A low-cost, large-area, and environment-friendly SERS-active substrate was acquired by sputtering inexpensive copper (Cu) on natural dragonfly wing (DW) with an easily controlled way of magnetron sputtering. By controlling the sputtering time of the fabrication of Cu on the DW, the performance of the SERS substrates was greatly improved. The SERS-active substrates, obtained at the optimal sputtering time (50 min), showed a low detection limit (10^{-6}M) to 4-aminothiophenol (4-ATP), a high average enhancement factor (EF, 1.98×10^4), excellent signal uniformity, and good reproducibility. In addition, the results of the 3D finite-difference time-domain (3D-FDTD) simulation illustrated that the SERS-active substrates provided high-density "hot spots", leading to a large SERS enhancement.

Keywords: surface-enhanced Raman scattering, dragonfly wing, copper, magnetron sputtering

PACS: 78.30.–j, 74.25.nd, 61.46.–w **DOI:** 10.1088/1674-1056/27/1/017801

1. Introduction

Surface-enhanced Raman scattering (SERS) is a very active area of research, that overcomes the general shortcomings of weak Raman scattering signals[1] and has been implemented in practical applications in environmental science studies,[2,3] trace detection,[4,5] medical biology,[6–9] and food safety testing.[10–16] SERS is a phenomenon whereby Raman scattering signals are strongly enhanced when molecules are absorbed onto a nanorough metal surface. It has also been confirmed that a relatively stronger SERS effect of SERS-active substrates is due to the strong coupling of local surface plasma resonances (LSPR) at metal nanorough surfaces causing local electromagnetic enhancement ("hot spot" areas).[17–19] This mechanism demonstrates electromagnetic (EM) enhancement, which is a main way of enhancement compared to change transfer (CT) enhancement. The LSPR of noble metals such as gold (Au), silver (Ag), and copper (Cu) cover most of the visible and near infrared wavelength range;[19–21] thus, these metals are often used for fabricating SERS substrates. Among these, Cu is not only the cheapest but also its SERS spectrum intensity can remain constant in time when probing molecules are adsorbed onto the Cu surface.[20–22] Therefore, we choose Cu as the metal material for our low-cost and high-performance SERS substrates.

Conventional methods for fabricating SERS-active substrates are based on the aggregation of colloidal nanoparticles, where these "hot spots" are random in quantity, dimension, and location.[17] To avoid this drawback, several other approaches have been proposed, such as self-assembly[23] and lithography techniques.[24] However, these substrates have modest SERS sensitivities.[17] The three-dimensional nanostructure arrays such as, silicon nanowire/nanopillar,[25] carbon nanotube,[26] and glass nanopillar,[27] dramatically increase the binding sites for probing molecules and the density of "hot spots".[17] Despite these advantages, the process of fabricating these templates is usually complicated. Moreover, the rigorous experimental conditions and expensive production costs also limit the practical applications of these SERS technologies.[28] The natural dragonfly wing (DW) is an excellent substrate material with an epicuticular layer composed of multi-column nanopillars, providing more binding sites for the absorption of probing molecules. Meanwhile, the surfaces of DWs are super hydrophobic,[29] making trace detection possible.

Many methods can be adopted to fabricate Cu nanoislands to the DW template. Magnetron sputtering, a physical deposition method with high speed, low temperature, and low damage, was developed in the 1970s.[30] Compared with traditional chemical deposition, the magnetron sputtering method has many outstanding merits in improving the fabrication efficiency and increasing the performance of SERS substrates. On the one hand, the Cu nanostructure obtained by magnetron sputtering is very uniform and the Cu coatings have high ho-

*Project supported by the Youth Fund Project of University Science and Technology Plan of Hebei Provincial Department of Education, China (Grant No. QN2015004) and the Doctoral Fund of Yanshan University, China (Grant No. B924).

†Corresponding author. E-mail: wml@ysu.edu.cn

© 2018 Chinese Physical Society and IOP Publishing Ltd

mogeneities and minimal impurities.[31] On the other hand, the adhesion of Cu to DWs is very strong and the properties of the Cu are not affected. Meanwhile, it is easy to operate the magnetron sputtering apparatus and the parameters in the process are controllable.[31–33]

In this paper, we deposited Cu nanoislands on natural DWs with magnetron sputtering to fabricate a low-cost, environment-friendly, and suitable for large-scale production SERS-active substrate. The vibrational characteristics and distributions of Raman peaks of rhodamine 6G (R6G) are well known as these have been thoroughly discussed in previous papers.[34–36] Therefore, R6G was chosen for the probing molecules to screen out the substrates with optimal performance. In addition, the 4-ATP was a bifunctional molecule in which the -SH group was easily cleaved to form a metal-S bond when absorbed onto a metal surface, and the protonated -NH_2 group could absorb on the metal surface through the electrostatic force.[37] By controlling the experimental conditions, it was possible for 4-ATP to form a single molecular layer on the metal surface.[37] Therefore, it was also selected as probing molecules to test the performance of our SERS substrates. Based on the analysis of massive experiment data, when the sputtering time of metal Cu was controlled at 50 min, the SERS substrates (Cu/DW substrates) achieved the strongest enhancement effect. Selecting random sets of experimental data to test the activity of SERS-active substrates with different concentrations of the 4-ATP solution, the value of detection limit (10^{-6} M) to 4-ATP was obtained. Additionally, the highest average EF reached 1.98×10^4 when the SERS substrates were used to detect 10^{-4} M 4-ATP.

2. Experimental

2.1. Materials and instruments

The DWs were purchased from Beijing Jiaying Grand Life Sciences Co., Ltd. The Cu (99.99%) target material was obtained from Nanchang Material Technology Co., Ltd. Both R6G and 4-ATP were procured from J&K Scientific LTD. Deionized water was acquired from Key Laboratory for Microstructural Material Physics of Hebei Province and was used throughout the experiment. The microstructures of the Cu/DW substrates and DWs were observed using a scanning electron microscope (Hitachi-3400) and the SERS spectra were obtained by a (inVia) Raman system. The DWs were decorated by Cu nanoislands with a radio frequency (RF) magnetron sputtering apparatus (DHRM-3).

2.2. Sample preparation

All the DWs were cleaned in acetone, ethanol, and deionized water for 20 min to get rid of the stain, followed by natural drying. Before sputtering, the preprocessed substrates were fixed on glass slides. Then the Cu nanoislands were deposited onto the DWs and the prepared SERS-active substrates were stored in a vacuum chamber soon afterwards to avoid surface oxidation. The procedure of forming different metal nanostructures on templates by magnetron sputtering system has the following steps. In the initial stage, atoms continually increase on the surface of the template forming groups. Gradually, these atom groups grow into "nuclei". After constantly absorbing new atoms, they grow to become a number of "islands". The uniting of one "island" with another "island" forms a network structure. Afterwards, the gaps on the network structure are gradually filled by subsequent atoms and thus the film is created. Figure 1 shows the top-view SEM image of a part of the DW whose epicuticular layer was composed of multi-column sloping pillars with average heights of ~200 nm. The approximate distance between the adjacent two pillars was 180±30 nm, and the diameter of these round tops was 80±20 nm. Based on the size parameters and the distribution of the pillars, as well as by controlling the sputtering time, Cu nanoislands were formed on the surface of the DW. Meanwhile, the Cu/DW substrates were fabricated and the distribution information of the Cu nanoislands on the pillars from Fig. 1, in which three types of "hot spots" were displayed. The adjacent Cu nanoislands on two neighboring pillars could produce "hot spots" (I). Adjacent Cu nanoislands on the same pillar could also form "hot spots" (II). The resonances of surface local plasma of Cu nanoislands themselves could form "hot spots" (III). Among them, the "hot spots" between the two adjacent nanoislands at the top of the pillars played a most important role in enhancing Raman intensities. In the experiment, while considering a variety of factors, the sputtering time of metal Cu was controlled at 30, 40, 50, 60, and 70 min, and in the following discussion the corresponding substrates are referred to as DW30, DW40, DW50, DW60, and DW70, respectively. During the deposition process, the sputtering rate was ~5 nm/min and the sputtering voltage was controlled at 90 V, with a current of 170 mA. The vacuum was 3.5×10^{-3} Pa, and the experiment was performed at room temperature.

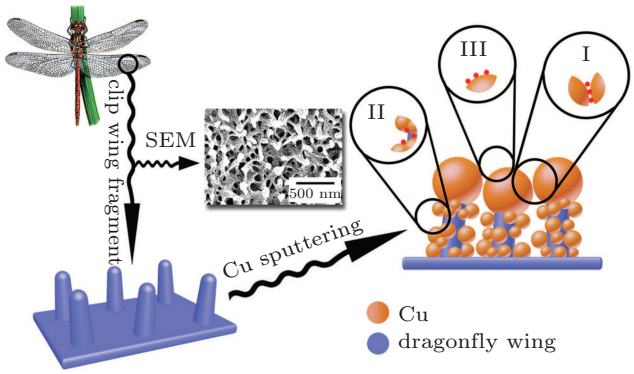


Fig. 1. (color online) Process of decorating Cu on DW. Top-view SEM image of a part of the DW shows that the surface of a DW is composed of multi-column sloping pillars.

2.3. SERS measurements

The surface information of the DWs with and without Cu nanoislands was examined using a scanning microscope. To screen out the optimal substrates from the prepared substrates with different Cu sputtering times, 10^{-3} M R6G droplets were added to these substrates and naturally evaporated. After screening, a few optimal substrates were immersed in 4-ATP ethanol solution with different concentrations for approximately 24 hours and then rinsed with pure ethanol to remove unbound 4-ATP. After that, the processed substrates were dried with nitrogen to ensure that a complete single molecule layer was formed on the surface of SERS substrate. Then, the activity of the optimal substrates could be tested. All of the Raman signals were acquired at room temperature in the Raman system with the 633 nm laser for excitation. By using the 633 nm laser the fluorescent interference was reduced and damage to the substrate avoided, enabling the preferred SERS enhancement. The diameter of the light spot area was ~1 μm and the spectral resolution was 1 cm^{-1}. In order to obtain reliable results, all data were acquired by selecting 20 random measurement results.

3. Results and discussion

3.1. Characterization

As in the SEM images (Fig. 2) of DWs with different Cu surface morpha, the top of the nanopillars became more regular after the Cu nanoislands were sputtered on them. Figures 2(a)–2(d) show the top-views of DW30, DW40, DW50, and DW70, with corresponding top diameters of the measured decorated pillars of 160±20 nm, 200±20 nm, 240±20 nm, and 280±20 nm, respectively. Because most of the DWs pillars were tilted, irregular in distribution, and even cross-distributed, almost all of the Cu nanoislands used the top of the pillars as base points to grow. As shown in Fig. 2(e), at the top of the pillars, not only were the Cu nanoislands large in size but also very regular in distribution, while the Cu nanoislands at the lower end of the pillars were small in size with irregular distributions. This is why the "hot spots" between the two neighboring nanoislands at the top of the pillars were the main "hot spots". For an increase in the sputtering time, the top diameter of the decorated nanopillars increased and the distance between adjacent decorated nanopillars decreased. With a large sputtering time of 70 min, the nanogaps were almost filled with Cu, leading to a sharp decline of the "hot spot" density between neighboring pillars. At the same time, the enhancement also reduced dramatically.

3.2. SERS performances and EF calculation

The SERS spectra of R6G on different SERS-active substrates (DW30, DW40, DW50, DW60, and DW70) were shown in Fig. 3(a) with the change of the Cu sputtering time,

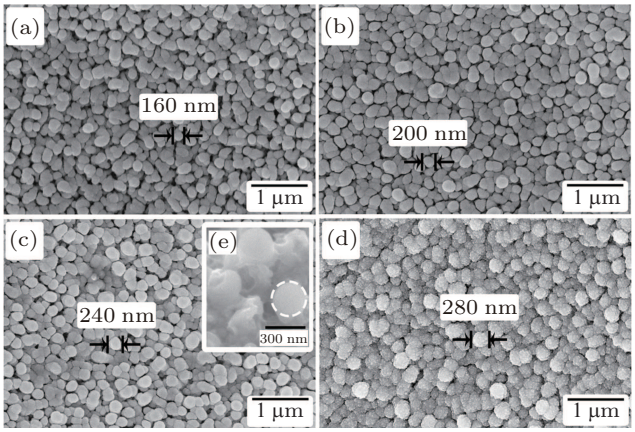


Fig. 2. (color online) (a)–(d) Top-view SEM images of DW30, DW40, DW50, and DW70, respectively. (e) Side-view SEM image of the DW50 substrate.

the intensities of SERS spectra changed significantly. It is obvious from Fig. 3(b) that compared with other SERS substrates, the DW50 substrate achieved the greatest enhancement effect. The several Raman characteristic peaks of the R6G molecules at 611, 772, and 1127 cm^{-1} were associated with C–C–C ring in-plane, out-to-plane bending, and C–H in-plane bending vibrations, respectively. The other characteristic peaks of 1190, 1360, 1509, 1572, and 1649 cm^{-1} were assigned to the stretching modes of aromatic C–C in-plane.[28,38] The SERS spectrum of 10^{-3} M 4-ATP on the DW50 substrate (A) and Raman spectrum of solid 4-ATP (B) are shown in Fig. 3(c). Compared with the Raman spectrum obtained in the solid, part of the Raman characteristic peaks of the SERS spectrum obtained in the Cu/DW substrate had a significant frequency shift. The Raman peak of 1087 cm^{-1} in Fig. 3(c) (B) was moved to 1080 cm^{-1} in Fig. 3(c) (A), similarly, 1593 cm^{-1} was shifted to 1576 cm^{-1}. These were the results of the reaction between the Cu surface and -SH group in the 4-ATP.[39] The shifted Raman characteristic peaks at 1005, 1080, 1191, 1474, and 1576 cm^{-1} correspond to the a_1 vibration mode, while the other characteristic peaks of 1149, 1309, 1380, and 1423 cm^{-1} correspond to the b_2 vibration mode as displayed in Table 1.[40] As shown in Fig. 3(d), the SERS spectrum intensity changed with the variation of 4-ATP concentration (from 10^{-2} to 10^{-6} M), maintaining obvious characteristic peaks of 4-ATP even at the concentration of 10^{-6} M. The fact that the Cu/DW substrate could reach such a detection limit was due to the super hydrophobicity of the surface of

Table 1. The vibration modes and relative standard deviation (RSD) corresponding to the different Raman characteristic peaks of 4-ATP.

Position of Raman peaks/cm^{-1}	Vibration modes	RSD
1005	a_1	8.27%
1080	a_1	6.71%
1149	b_1	6.85%
1191	a_1	6.19%
1309	b_1	6.06%
1380	b_1	7.72%
1423	b_1	7.08%
1474	a_1	5.63%
1576	a_1	5.92%

the DWs to a certain extent.[41] The Raman signal intensities of 4-ATP at 25 randomly selected positions from 5 different DW50 substrates are shown in Fig. 3(e) which illustrates the reproducibility of our SERS-active substrates. The point-by-point SERS mapping using a randomly selected 5×5 μm^2 area with a step size of 1 μm is shown in Fig. 3(f), in which each brightness of the grid represents the intensity of the SERS signal. The relatively uniform color distribution indicated that the signal intensities of the testing area were more uniform, further illustrating the homogeneity over the entire area of our DW50 substrates. In addition, each relative standard deviation (RSD) of the signal intensity of 10^{-3} M 4-ATP corresponding to the different Raman characteristic peaks was calculated below 10% and exhibited in Table 1. These results show an excellent repeatability and uniformity for the DW50 substrates.

For calculating the SERS EF of the DW50 substrate, we used the following formula:[40]

$$\mathrm{EF} = (I_{\mathrm{surf}}/I_{\mathrm{bulk}}) \times (N_{\mathrm{bulk}}/N_{\mathrm{surf}}), \tag{1}$$

where I_{surf} and I_{bulk} are the intensity of the Raman peak in the SERS and Raman spectra, respectively. We choose the peak centered at 1080 cm^{-1} for the a_1 vibration mode. N_{bulk} and N_{surf} are the numbers of the 4-ATP molecules in the bulk solid sample and surface of DW50 substrates, respectively. The value of I_{surf} ($\sim 1.15 \times 10^5$) is obtained after 4-ATP

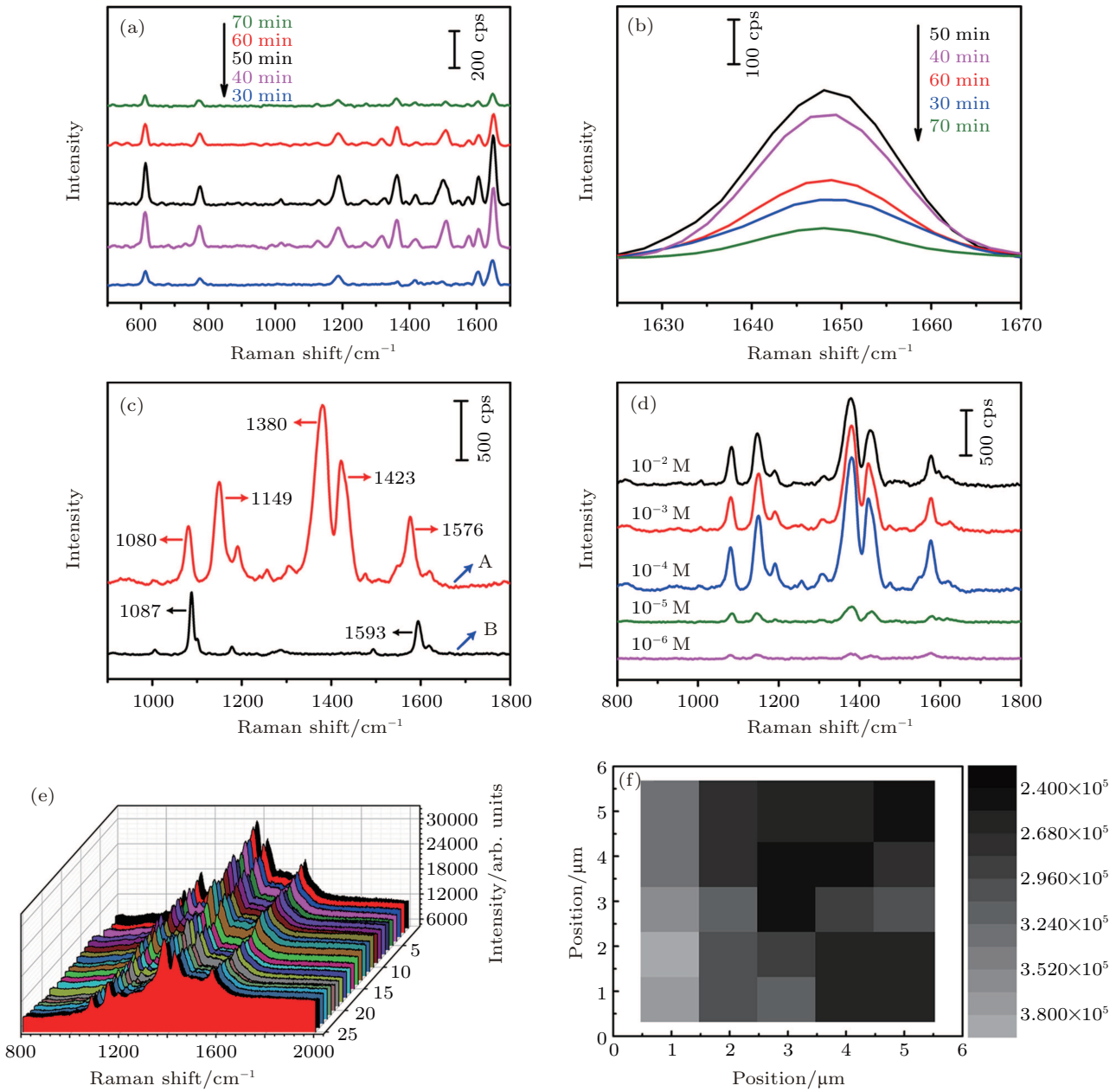


Fig. 3. (color online) (a) SERS spectra of 10^{-3} M R6G on different SERS substrates (DW30, DW40, DW50, DW60, and DW70). (b) A comparison of the intensity of Raman characteristic peak in image (a) at 1649 cm^{-1} between different SERS-active substrates. (c) SERS spectrum of 10^{-4} M 4-ATP on the DW50 substrate (A) and Raman spectrum of solid 4-ATP (B). (d) SERS spectra of 4-ATP for different concentrations on the substrate of DW50. (e) SERS spectra of 4-ATP at the concentration of 10^{-3} M on 25 randomly selected positions of the DW50 substrates. (f) SERS mapping (5×5 μm^2, 1 μm step size) of the characteristic peak of 4-ATP at 1380 cm^{-1} on the DW50 substrates.

molecules form a monolayer on the DW50 substrate. The corresponding I_{bulk} (calculated from the solid 4-ATP sample) is $\sim 5.46 \times 10^4$. Therefore, the ratio I_{surf}/I_{bulk} is equal to ~2.11 ($1.15 \times 10^5/5.46 \times 10^4$). For the solid 4-ATP sample, N_{bulk} can be determined by[40]

$$N_{bulk} = V\rho N_A/M, \tag{2}$$

where ρ (1.18 g/cm^3) and M (125.19 g/mol) represent the density and molecular weight of 4-ATP, respectively, and N_A ($\sim 6.022 \times 10^{23}$) is Avogadro's number. V is the collection volume of the solid sample monitor in which the diameter of the illumination focus is about 1 μm and the penetration depth of the 633 nm laser beam is ~ 10 μm in our Raman setup. Therefore, the calculated values of V and N_{bulk} are ~ 7.85 μm^3 and $\sim 4.46 \times 10^{10}$, respectively. When we calculate N_{surf}, the 4-ATP molecules adsorbed onto the surface of SERS substrate are considered to be a single layer. In addition, the surface area of one 4-ATP molecule is ~0.2 nm^2.[37] Considering the surface morpha of the topmost Cu nanoislands on the substrates, the illumination area is calculated as ~1.57 μm^2. Therefore, the obtained value of N_{serf} is 7.85×10^6. We obtain a ratio N_{bulk}/N_{serf} of 5.68×10^3 ($4.46 \times 10^{10}/7.85 \times 10^6$). According to formula (1), the EF of the DW50 substrate is 1.98×10^4.

3.3. 3D finite-different time-domain simulation

The 3D finite-different time-domain (3D-FDTD) simulation is a well-known simulation method that can be used to analyze the spatial distribution of local electric fields amplifying the Raman signal on noble metal nanorough surfaces. Figure 4(a) shows the structural model of the DW50 substrate, where Cu nanoislands are decorated on the pillars and the calculated planes are exhibited in Fig. 4(b). Moreover, the upper diameter of every decorated pillar is 240 nm. A rectangular-shaped continuous wave laser with a wavelength of 633 nm is shot along the K direction toward the structure and the polarization direction of the laser is in the E direction. Figures 4(c) and 4(d) display the spatial distribution of the electric field intensity for the x–y and x–z planes, respectively, defined in Fig. 4(b). Clearly, the main"hot spots" ("hot spots" I) are generated between the adjacent Cu nanoislands at the top of the pillars and "hot spots" II and III are modest in terms of the electric field intensity. Meanwhile, we focused on the surface morpha, structure and size of the Cu nanoislands decorated on the SERS substrates in the simulation to emphatically reflect the EM enhancement effect.[42] Furthermore, according to the relationship of the Raman enhancement scales and local field,[43] we get

$$G_{SERS} \approx [E_{loc}(\omega_{exc})/E_{inc}(\omega_{exc})]^4. \tag{3}$$

The parameters $E_{loc}(\omega_{exc})$ and $E_{inc}(\omega_{exc})$ are E and E_0 in the FDTD calculation, respectively. In our simulation, the maximum value of the calculated electric field is ~11.34 V·m^{-1}. Therefore, the theoretical EF (1.65×10^4) obtained is close to our experimental value. Moreover, the substrate structure is the main object of study in the simulation, and the probing molecules are not considered.

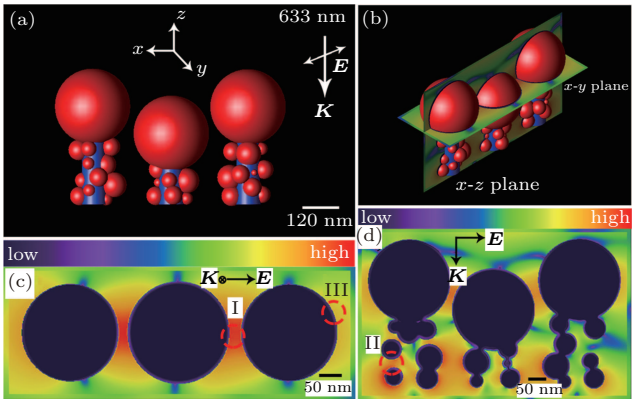


Fig. 4. (color online) (a) The FDTD model of the DW50 substrate. (b) The calculated planes. (c) and (d) Spatial distributions of the electric field intensity for the x–y and x–z planes, respectively, defined in (b).

4. Conclusion

A low-cost, large-area, and environment-friendly SERS-active substrate of Cu/DW with EF (1.98×10^4) and detection limit (10^{-6} M) for 4-ATP was fabricated by decorating Cu nanoislands on the natural DW. The high-density "hot spots" between neighboring Cu nanoislands at the top of pillars greatly improved the activity of our DW50 substrate, also supported by the 3D-FDTD simulation. Cu was used in our experiment, not only because it is the cheapest compared to other noble metals, but its SERS intensity remained constant in time when probing molecules were adsorbed onto the Cu surface. Meanwhile, DWs is an environment-friendly biological material which could be easily obtained from nature. Therefore, the SERS-active substrate of Cu/DW has prominent advantages in being widely applied in the practical detection of organic molecules.

References

[1] Lv M Y, Teng H Y, Chen Z Y, Zhao Y M, Zhang X, Liu L, Wu Z L, Liu L M and Xu H J 2015 *Sens. Actuators B Chem.* **209** 820
[2] Hao J, Han M J, Han S, Meng X, Su T L and Wang Q K 2015 *Environ. Sci.* **36** 152
[3] Dasary S S, Zones Y K, Barnes S L, Ray P C and Sing A K 2016 *Sens. Actuators B Chem.* **224** 65
[4] Lei O Y, Hu Y W, Zhu L H, Gary J C and Joseph I 2017 *Biosens. Bioelectron.* **92** 755
[5] Liu J, Zhou J, Tang B, Zeng T, Li Y L, Li J L, Ye Y and Wang X G 2016 *Appl. Surf. Sci.* **386** 296
[6] Fang H, Yin H J, Lv M Y, Xu H J, Zhao Y M, Zhang X, Wu Z L, Liu L and Tan T W 2015 *Biosens. Bioelectron.* **69** 71
[7] Liu Y, Zhou H, Hu Z, Yu G, Yang D and Zhao J 2017 *Biosens. Bioelectron.* **94** 131
[8] Qu L L, Liu Y Y and He S H 2015 *Biosens. Bioelectron.* **77** 292
[9] Tan Y Y, Yan B, Xue L L, Li Y, Luo X Y and Ji P 2017 *Lipids Health Dis.* **16** 73
[10] Polly L, Francois X N, Fanbin K, Azlin M and Mengshi L 2017 *Carbohydr. Polym.* **157** 643
[11] Li R P, Yang G H, Yang J L, Han J H, Liu J H and Huang M J 2016 *Food Control* **68** 14

[12] He S, Xie W, Zhang W, Zhang L, Wang Y, Liu X, Liu Y and Du C 2015 *Spectrochim. Acta Part A* **137** 1092
[13] Rajapandiyan P, Tang W L and Yang J 2015 *Food Control* **56** 155
[14] Fang H, Zhang X, Zhang S J, Liu L, Zhao Y M and Xu H J 2015 *Sens. Actuators B Chem.* **213** 452
[15] Qi M, Huang X, Zhou Y, Zhang L, Jin Y, Peng Y, Jiang H and Du S 2016 *Food Chem.* **197** 723
[16] Samir K, Pratibha G and Jitendra P S 2017 *Sens. Actuators B. Chem.* **241** 577
[17] Shao F, Lu Z C, Liu C, Han H Y, Chen K, Li W T, He Q G, Peng H and Chen J N 2014 *Acs. Appl. Mater. Interfaces* **6** 6281
[18] Ward D R, Grady N K, Levin C S, Halas N J, Wu Y, Nordlander P and Natelson D 2007 *Nano Lett.* **7** 1396
[19] Sharma B, Frontiera R R, Henry A I, Ring E and van Duyne R P 2012 *Mater. Today* **15** 16
[20] Kudelskia A, Bukowskaa J, Janik-Czachorb M, Grochalaa W, Szummerc A and Dolatab M 1998 *Vib. Spectrosc* **16** 21
[21] Jiji S G and Gopchandran K G 2017 *Spectrochim. Acta Part A* **171** 499
[22] Kudelski A and Bukowska J 1996 *Vib. Spectrosc.* **10** 335
[23] Wang J, Sun C S, Liu X F, Xin L L and Fang Y 2014 *Colloids Surf. A* **455** 104
[24] Dinish U S, Yaw F C, Agarwal A and Olivo M 2011 *Biosens. Bioelectron.* **26** 1987
[25] Wang M L, Zhang C X, Wu Z L, Jing X L and Xu H J 2014 *Chin. Phys. B* **23** 547
[26] Sharma H, Agarwal D C, Shukla A K, Avasthi D K and Vankar V D 2013 *Raman Spectrosc.* **44** 12
[27] Oh Y J and Jeong K H 2012 *Adv. Mater.* **24** 2234
[28] Guo L, Zhang C X, Deng L, Zhang G X and Xu H J 2014 *Appl. Phys.* **115** 213101
[29] Rajabi H and Darvizeh A 2013 *Chin. Phys. B* **22** 738
[30] Chen Y and Fang Y 2008 *Spectrochim. Acta Part A* **69** 733
[31] Lan M M, Li H Q, Wang D, Li Y and Xu G Y 2014 *Vacuum* **110** 87
[32] Wang X B, Song C, Geng K W, Zeng F and Pan F 2007 *Appl. Surf. Sci.* **253** 6905
[33] Voevodin A A, Rebholz C, Schneider J M, Stevenson P and Matthews A 1995 *Surf. Coat. Technol.* **73** 185
[34] Sharma H S S, Carmichael E and Call D M 2016 *Vib. Spectrosc.* **83** 159
[35] Li H, Jiang J, Wang Z, Wang X, Liu X, Yan Y and Li C 2017 *Colloid Interface Sci.* **501** 86
[36] Hao Z, Mansuer M, Guo Y, Zhu Z and Wang X 2016 *Talanta* **146** 533
[37] Wang Y L, Chen H J, Dong S J and Wang E K 2006 *Chem. Phys.* **124** 163
[38] Tsai Y C, Hsu P C, Liu Y W and Wu T M 2009 *Sens. Actuators B Chem.* **138** 5
[39] Wei G, Wang L, Liu Z G, Song Y H, Sun L L, Yang T and Li Z 2005 *Phys. Chem. B* **109** 23941
[40] Hong G S, Li C and Qi L M 2010 *Adv. Funct. Mater.* **20** 3774
[41] De A F, Gentile F and Mecarini F 2011 *Nat. Photon.* **5** 682
[42] Yang J L, Li R P, Han J H and Huang M J 2016 *Chin. Phys. B* **25** 083301
[43] García-Vidal F J and Pendry J B 1996 *Phys. Rev. Lett.* **77** 1163